^{1}H NMR, ^{31}P NMR and Raman Study of $CaHPO_4$ and $SrHPO_4$

B. Louati, K. Guidara, M. Gargouri, and M. Fourati

Laboratoire de l'état solide, Faculté des sciences de Sfax, BP 802, 3018 Sfax, Tunisia

Reprint requests to Dr. B. L.; E-mail: bassem_louati@yahoo.fr

Z. Naturforsch. **60a,** 121 – 126 (2005); received September 8, 2004

$CaHPO_4$ and $SrHPO_4$ were investigated using Raman, ^{1}H NMR and ^{31}P NMR techniques to study the environment of their PO_4^{3-} tetrahedra and the percentage of mobile protons. ^{1}H NMR spectra at room temperature suggest the presence of three types of protons, in agreement with RX investigation. The percentage of mobile protons in $SrHPO_4$ is greater than in $CaHPO_4$ because Sr^{2+} is bigger than Ca^{2+}. ^{31}P NMR spectra at room temperature show two lines in the spectrum of $SrHPO_4$, revealing an equal environment of two sets of pairs of PO_4^{3-}. The ^{31}P NMR spectrum of $CaHPO_4$, however, exhibits three lines. This result was confirmed using a cross polarization (CP) sequence program. The first peak is attributed to the first set of pairs of $P(1)O_4$ units and the two other ones to $P(2)O_4$ and $P(2')O_4$ units.

Key words: Raman Spectroscopy; ^{1}H and ^{31}P NMR Investigation.

1. Introduction

Hydrogen phosphates (HPO_4^{2-}) of alkaline earth metals, like brushite ($CaHPO_4{\cdot}2H_2O$), monetite ($CaHPO_4$), $SrHPO_4$ [1 – 3], are applied in protonic conductors, batteries and fuel cells. $CaHPO_4$ has also biological importance in the formation of bones and teeth. At 642 K it exhibits an irreversible transformation to the diphosphate ($P_2O_7^{4-}$) [4].

In the present paper the influence of the size of Ca^{2+} and Sr^{2+} is studied by means of ^{1}H and ^{31}P NMR measurements at room temperature.

2. Experimental

The alkaline earth hydrogen phosphates $AHPO_4$ (A = Ca, Sr) were obtained by the following spontaneous reaction at room temperature:

$$A(NO_3)_2 + NH_4H_2PO_4 \rightarrow AHPO_4 + 2NO_3^- + NH_4^+ + H^+.$$

Slow evaporation of the solution led to the formation and precipitation of the compounds. The powders were warmed at 353 K for a few hours to eliminate the humidity.

The samples were characterized by their X-ray powder patterns using a Philipps powder diffractometer with a CuK_α radiation source. All the X-ray peaks were indexed in the triclinic system with space group $P\bar{1}$ indicating a single phase corresponding to the anhydrous form: $a = 6.91(1)$ Å, $b = 6.63(3)$ Å, $c = 6.99(3)$ Å, $\alpha = 96.32°$, $\beta = 103.87°$, $\gamma = 88.37°$, $V = 309.29$ Å^3 for $CaHPO_4$ and $a = 7.19(1)$ Å, $b = 6.79(3)$ Å, $c = 7.25(3)$ Å, $\alpha = 94.66°$, $\beta = 104.96°$, $\gamma = 88.79°$, $V = 341.70$ Å^3 for $SrHPO_4$ (Fig. 1). The unit cell parameters agree well with the literature values [2, 3].

We note a little increase in the unit cell volume of $SrHPO_4$ in comparison to $CaHPO_4$, due to the difference between the ionic radii: $r(Sr^{2+}) > r(Ca^{2+})$.

3. Characterization of $AHPO_4$ compounds

3.1. Vibrational Study at Room Temperature

The regular PO_4^{3-} tetrahedra exhibit T_d symmetry with four independent vibrational bonds. These bonds are $\nu_1 - \nu_4$ of symmetry A_1, E, F_2 and F_2, respectively. The addition of protons to the anionic group reduces the symmetry from T_d to C_s and the number of independent vibrational modes changes to 12. Nine modes among them come from the bonds $\nu_1 - \nu_4$ of the PO_4^{3-} group. The three other bonds are linked to vibrations of the OH group and are denoted as ν(O-H), δ(O-H) and γ(O-H).

However, in the crystal all these vibrations disintegrate into several components because of the effect

Table 1. Factor group analysis of $CaHPO_4$ and $SrHPO_4$ at room temperature.

Irreducible representations of the C_i group	Internal modes HPO_4^{2-}	External modes HPO_4^{2-}	Activity
A_g	12	6	Raman
A_u	12	6	IR

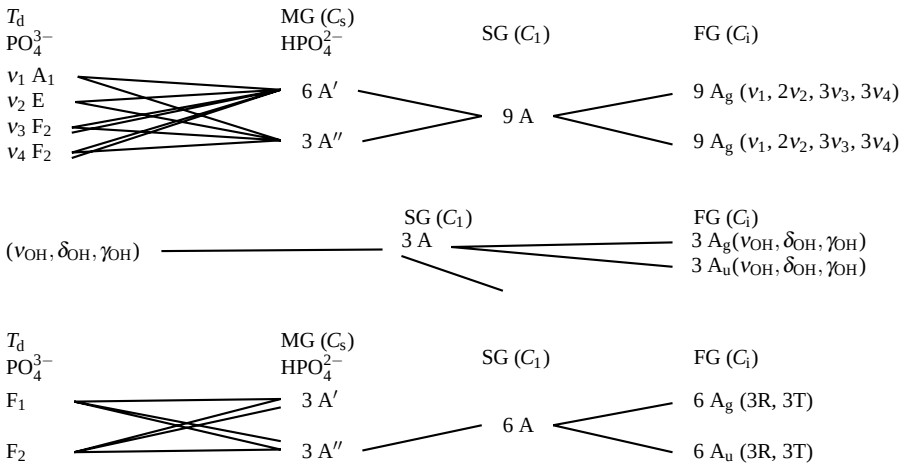

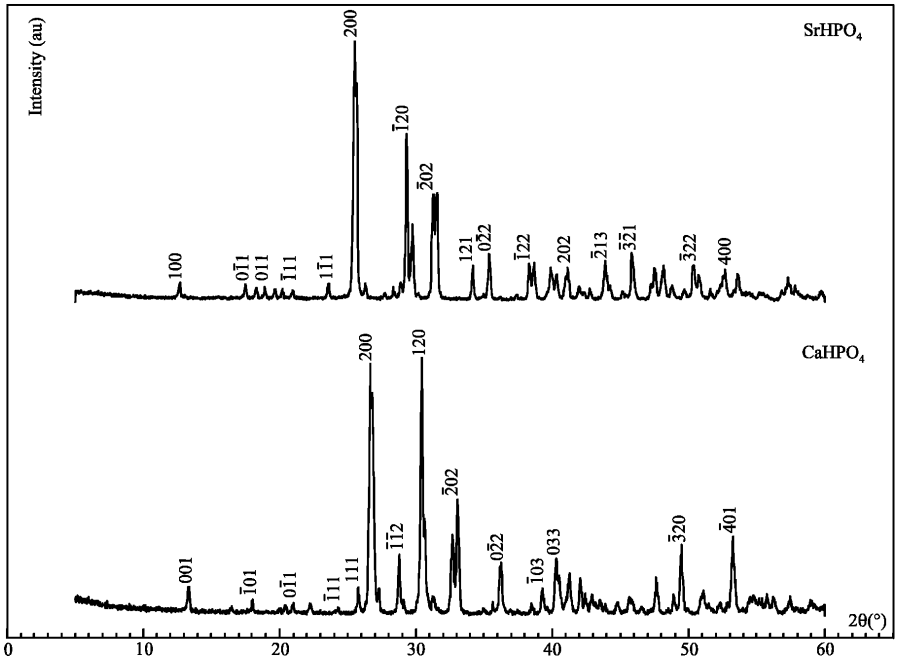

Fig. 1. X-ray diffractogram of $CaHPO_4$ and $SrHPO_4$ in the range 5° to 60°.

of the crystalline field. The correlation between the molecular group T_d, the site group C_1 and the factor group C_i shows that each molecular vibration splits into two components of symmetry A_g and A_u, which are Raman and IR active. The effect of going from the site group to the unit cell group is to cause splittings of the free molecule frequencies. The total number of external lattice modes of $CaHPO_4$ and $SrHPO_4$ is 6 A_g + 6 A_u, while that of the internal motions is 12 A_g + 12 A_u, coming from the contribution of the PO_4^{3-} and OH group. The number of external and internal modes anticipated by the factor group analysis is

Table 2. Observed Raman frequencies (in cm^{-1}) for $AHPO_4$.

$CaHPO_4$	$SrHPO_4$		Assignments
380, 410	385, 410	s	ν_2(P-O)
555, 585	555, 575	s	ν_4(P-O)
900	890	s	ν(P-OH)
985	990	Vs	ν_1(P-O)
1090, 1130	1095, 1140	w	ν_3(P-O)

Vs = very strong; s = strong; w = weak.

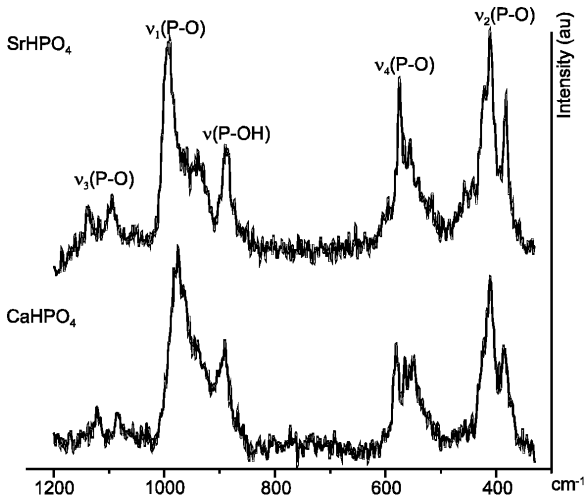

Fig. 2. Raman spectra at room temperature for $CaHPO_4$ and $SrHPO_4$.

higher than observed in the Raman spectra of $CaHPO_4$ and $SrHPO_4$ (Table 1).

The Raman spectra of $AHPO_4$ sealed in glass tubes were obtained in the range 300 – 1200 cm^{-1} employing a RTI 30 Dilor instrument triple monochromator using the 514.5 nm line of a Spectra Physics argon ion laser (Fig. 2). The wave numbers agree with those reported in [5 – 7], but with some minor differences (Table 2). The internal vibrational bonds can be divided into two parts: 1) vibrational modes of the PO_4^{3-} anions; 2) vibrational modes of the P-OH in the vicinty of 900 cm^{-1}.

3.2. Vibration of PO_4^{3-} Anions

In the Raman spectrum the bonds observed in the (380 – 410 cm^{-1}) and (555 – 585 cm^{-1}) frequency ranges are assigned to ν_2(P-O) and ν_4(P-O) modes of the tetrahedral PO_4 groups. The bending band seen above 990 cm^{-1} can be interpreted as the ν_1(P-O) modes. On the other hand, the weak bands at 1090 – 1140 cm^{-1} correspond to the ν_3(P-O) vibration modes of the tetrahedral PO_4 groups.

Table 3. Experimental conditions.

	^{1}H	^{31}P (ZG MAS)	^{31}P (CP MAS)
Pulse length [μs]	16.65	15.6	15.6
Dead time [μs]	7	10	10
Recycle time [s]	1	5	2
Resonance frequency [MHz]	300.13	121.49	121.49
MAS spinning speed [Hz]	Static	8000	8000
Number of scans	128	720	32832
Number of digitised points	6002	4096	4096
Referencing 0 Hz	TMS	H_3PO_4 (85%)	H_3PO_4 (85%)

Table 4. Deconvolution parameters of $SrHPO_4$ (+) and $CaHPO_4$ ($*$).

Name	Lineshape	Position ($\pm$0.5 ppm)	Line width ($\pm$0.5 ppm)	Normalized area (%)
P_1	Gauss	3.9^{+}	21.6^{+}	33^{+}
		2.2^{*}	26.1^{*}	42.5^{*}
P_2	Lorentz	6^{+}	4.9^{+}	21.2^{+}
		4.4^{*}	10.5^{*}	12.7^{*}
P_3	Gauss	22.8^{+}	22.7^{+}	45.8^{+}
		22.6^{*}	23.9^{*}	44.8^{*}

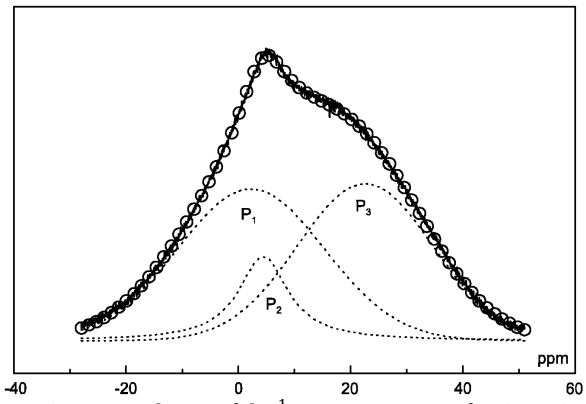

Fig. 3. Deconvolution of the ^{1}H NMR spectrum for $CaHPO_4$ at room temperature.

The Raman study suggests the presence of a mobile proton corresponding to the long (O-H-O) length in the structure. In order to determine the percentage of this mobile proton, we have undertaken the ^{1}H NMR study of $AHPO_4$.

The ^{1}H NMR experiments were performed on a Bruker MSL 300 ($B = 7.1$ T) spectrometer.

A zero go (ZG) sequence program has been used. The NMR acquisition conditions are reported in Table 3.

For $CaHPO_4$ the ^{1}H NMR spectrum at room temperature is characterized by the presence of three peaks, P_1, P_2, and P_3. The simulation is realized by mixing

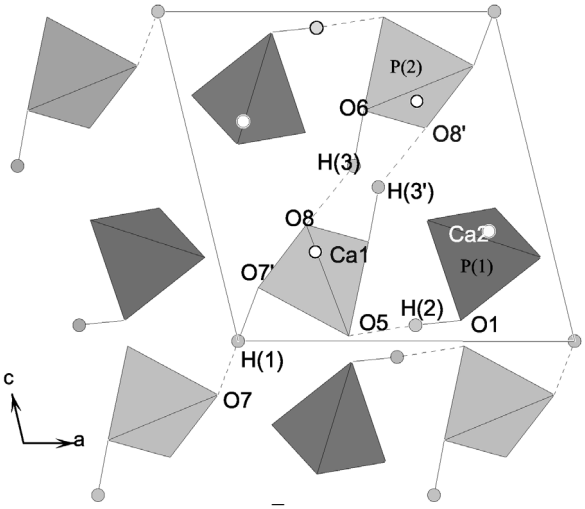

Fig. 4. [010] view of the $P\bar{1}$ structure of $CaHPO_4$, emphasizing the hydrogen-bonding schema and the PO_4 tetrahedra pattern.

two Gaussian functions for the P_1 and P_3 peaks and a Lorentzian function for the P_2 peak, revealing the existence of three types of protons in the structure (Table 4). The dotted lines in Fig. 3 present the Gaussian and Lorentzian peaks. The P_2 peak represents the H^+ ions that are mobile at room temperature, while P_1 and P_3 represent two types of fixed protons involving different local surroundings of PO_4^{3-} groups.

The ^{1}H NMR study agrees with the structural study. In fact, at room temperature $CaHPO_4$ presents an average $P\bar{1}$ structure with two distinct sets of pairs of PO_4 units and three types of hydrogen bonds. One proton, H(1), centred on a symmetric hydrogen bond, O(7)-H(1)…O(7'), with O(7)…O(7') = 2.458(2) Å. The second hydrogen atom H(2) of the structure is on an usual hydrogen bond, O(1)-H(2)…O(5), with O(1)…O(5) = 2.565(1) Å. The third H(3) is disordered over two centrosymmetrically related positions, O(6)-H(3)…O(8), where O(6)…O(8) = 2.669(1) Å, but is presumed to be statistically disordered with hydrogen atoms covalently bonded to half of the O(6) atoms on average [8].

The disorder is assumed to be static, because H(3)…H(3') = 1.7 Å seems to be too long for dynamic effects. Two configurations should show H(3) bonded to O(6) only and to O(6') only, respectively (Fig. 4).

Based on the structural study, the ^{1}H NMR investigation let us to deduce the following results:

i) The P_2 peak, attributed to the H^+ ion, is assigned to the disordered hydrogen H(3).

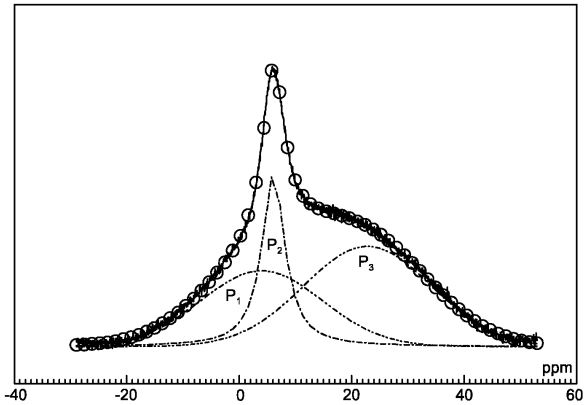

Fig. 5. Deconvolution of the ^{1}H NMR spectrum for $SrHPO_4$ at room temperature.

ii) The H(1) and H(2) protons with the shortest O-H-O lengths are the species presented by the two Gaussian functions (fixed proton).

For the given temperature, the fixed and mobile proton numbers are proportional to the areas of the Gaussian and Lorentzian peaks, respectively. The percentage of mobile protons is

$$\frac{100\% \cdot P_2}{P_1 + P_2 + P_3} \cong 12.7\%.$$

Concerning $SrHPO_4$, the deconvolution of the spectrum is also realized by mixing of three functions (Fig. 5); two Gaussian functions of the P_1 and P_3 peaks and one Lorentzian function of the P_2 peak (Table 4). The percentage of mobile H^+ ions is 21.2%.

Table 4 reveals that the P_3 peak deduced from the deconvolution of the ^{1}H NMR spectrum of $CaHPO_4$ has the same position as that observed in the $SrHPO_4$ spectrum, in spite of the different cation sizes. However, a small variation in the position of P_1 and P_2 peaks is observed. Besides we note a little increase in the percentage of mobile protons of $SrHPO_4$ in comparison with $CaHPO_4$ due to the difference in the ionic radii: $r(Sr^{2+}) > r(Ca^{2+})$.

3.3. ^{31}P NMR Investigation

In order to study the PO_4^{3-} tetrahedron and to determine the influence of the A cation size, we have undertaken a ^{31}P NMR investigation of $AHPO_4$ at room temperature. The ^{31}P NMR experiments were performed on a Bruker MSL 300 ($B = 7.1$ T) spectrometer working at 121.49 MHz. A high speed probe with 5 mm rotors spinning at 8000 Hz has been used. A ZG (zero go)

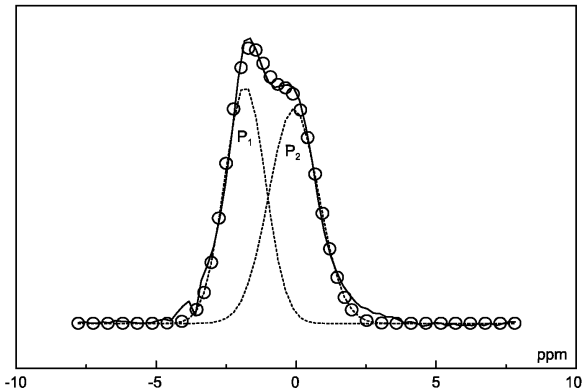

Fig. 6. Deconvolution of the ^{31}P NMR spectrum of $SrHPO_4$ at room temperature.

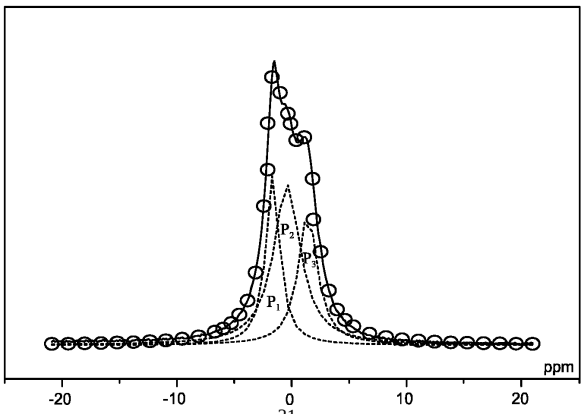

Fig. 7. Deconvolution of the ^{31}P NMR spectrum of $CaHPO_4$ at room temperature.

sequence program was used with a $\pi/2$ pulse length of 3 μs. The NMR acquisition conditions are reported in Table 3.

Figures 6 and 7 represent the ^{31}P NMR spectra of the samples with a spinning rate $\omega = 8$ kHz using a ZG sequence program. The $SrHPO_4$ spectrum is characterized by two large peaks (Fig. 6). It can be totally simulated with two Gaussian functions having equal intensities, revealing the presence of two distinct sets of pairs of PO_4 tetrahedra (Table 5). This result agrees well with a structural study [3].

Concerning $CaHPO_4$, three Lorentzian functions are necessary to simulate the spectrum. Figure 7 represents the ^{31}P NMR spectrum of the sample; it is characterized by three peaks A, B and C at the positions -1.6, -0.4 and 1.4 ppm in proportions 1/4, 1/2 and 1/4, respectively (Table 5).

It should be noted that the chemical shift of the ^{31}P MAS NMR peaks corresponding to $CaHPO_4$ agree

Table 5. Deconvolution parameters of the ^{31}P NMR spectrum of $SrHPO_4$(+) and $CaHPO_4$ [( ), ZG MAS sequence program; (∗), CP MAS sequence program).

Function	P_1	P_2	P_3
	(-1.6)	(-0.4)	(1.4)
Position (±0.5 ppm)	-1.58^*	-0.3^*	1.37^*
	-1.8^+	0^+	
Normalized area (%) (ZG MAS)	(25.5)	(47.4)	(27.1)
	47.6^+	52.4^+	
Line width (±0.5 ppm) (ZG MAS)	(1.4)	(2.8)	(1.9)
	1.4^+	1.7^+	

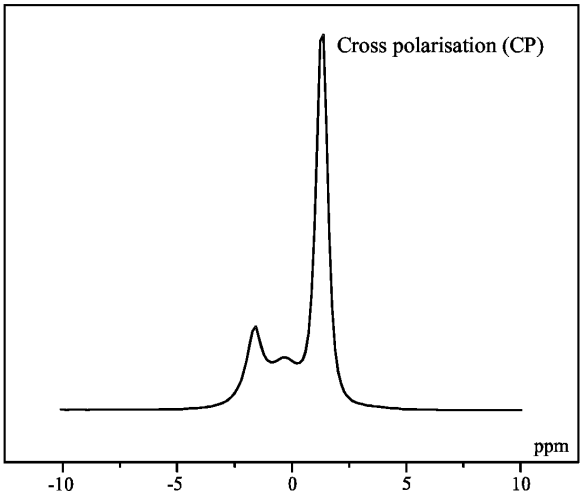

Fig. 8. ^{31}P NMR MAS spectrum at room temperature for $CaHPO_4$.

with the observations by several authors on different apatites [9–11] and with the known hydroxyapatites [e.g. $Sr_{10}(PO_4)_6(OH)_2$, $Pb_{10}(PO_4)_6(OH)_2$], δ_{iso} of which is in the range -0.7 to 2.9 ppm [12–14].

The ^{31}P NMR spectrum of $CaHPO_4$ reveals the presence of three distinct environments of PO_4^{3-}. In order to enhance the multinuclear signal intensities, cross polarization (CP), involving the transfer of magnetization from abundant nuclei, usually from protons, to the dilute nuclei (*e.g.* ^{31}P, ^{13}C, ^{29}Si), which also reduces the recycle delays, can be used. The ^{31}P CP MAS spectra were obtained by means of the standard cross-polarization pulse technique followed by ^{1}H high-power decoupling. For the recorded spectrum, a contact time of 1 ms and a period between successive accumulations of 2 s were chosen. The number of scans was 32832 (Table 3). The CP NMR pattern is obviously characterized by the presence of three peaks placed at -1.58, -0.3 and 1.37 ppm (Fig. 8 and Table 5). This result matches well with the previously reported results and confirms the presence of three phos-

phorus sites observed in the spectrum recorded using the ZG sequence program.

The ^{31}P NMR investigation revels the presence of three phosphorus sites. This result seems to disagree with the structural study. In fact, only two distinct sets of pairs of PO_4 units are found in the primitive cell by X-ray investigation. We have therefore revised the structural study of $CaHPO_4$ crystal.

H(3) is presumed to be statistically disordered with hydrogen covalently bonded to half of the O(6) atoms on average. Two configurations should, respectively, show H(3) bonded to O(6) only and to O(6') only. The two tetrahedra of P(2) and P(2') are inequivalent, so, when H(3) links to one of them, the two different groups HPO_4^{2-} and $H_2PO_4^{-}$ are formed in the structure. The HPO_4^{2-} and $H_2PO_4^{-}$ entities are inequivalent. This results in the apparition of two distinct peaks in the ^{31}P NMR spectrum.

Based on the revised structural study, the observed spectrum (Fig. 6) can be explained:

i) The B peak is attributed to the first set of pairs of $P(1)O_4$ units.

ii) The A and C peaks correspond to P(2) and P(2') tetrahedra with equal proportions 1/4, respectively.

4. Conclusion

In this work we have synthesized $AHPO_4$ (A = Ca, Sr). These samples were investigated by X-ray diffraction, Raman, ^{1}H and ^{31}P NMR spectroscopy.

The Raman study suggests proton mobility along the long O-H-O length in the structure. The ^{1}H NMR investigation of $AHPO_4$ has allowed the determination of 12.68% mobile protons for $CaHPO_4$ and 21.19% for $SrHPO_4$. The ^{31}P NMR investigation suggested two different phosphorus environments in $SrHPO_4$ and three in $CaHPO_4$. The first peak is attributed to the first set of pairs of $P(1)O_4$ units and the two resting peaks correspond to $P(2)O_4$ and $P(2')O_4$ tetrahedra.

[1] G. R. Sivakumar, E. K. Girija, S. N. Kalkura, and C. Subramanian, Cryst. Res. Technol. **33**, 197 (1998).
[2] B. Dickens, J. S. Bowen, and W. E. Brown, Acta Cryst. **B28**, 797 (1971).
[3] A. Boudjada, R. Masse, and J. C. Guttel, Acta Cryst. **B34**, 2692 (1978).
[4] R. A. Vargas and M. Mosquera, Rev. Mex. Fis. **3**, 450 (1993).
[5] J. Xu, I. S. Butler, and D. Gilson, Spectrochim. Acta **A55**, 2801 (1999).
[6] K. Nakamoto, Infrared and Raman Spectra of Inorganic and Coordination Compounds, John Wiley and Sons, New York 1997.
[7] M. G. Taylor, K. Simkiss, S. F. Parker, and P. C. H. Mitchell, Phys. Chem. Chem. Phys. **1**, 3141 (1999).
[8] M. Catti and G. Ferraris, Acta Cryst. **B33**, 1223 (1977).
[9] J. L. Miquel, L. Facchini, A. P. Legrand, X. Marchandise, P. Lecouffe, M. Chavanaz, M. Donozzan, C. Rey, and J. Lemaître, Clin. Mater. **5**, 111 (1990).
[10] J. P. Yesinovski and H. Eckert, J. Am. Chem. Soc. **109**, 6274 (1987).
[11] A. Rodrigues and A. Lebugle, Colloids and Surfaces (A): Physicochemical and Engineering Aspects. **145**, 191 (1998).
[12] J. P. Yesinowski, J. Am. Chem. Soc. **103**, 6266 (1981).
[13] B. Badraoui, M. Debbabi, R. Thouvenot, and C. R. Hebd, Acad. Sci. Ser. IIC. **3**, 107 (2000).
[14] B. Badraoui, A. Bigi, M. Debbabi, M. Gazzano, N. Roveri, and R. Thouvenot, Eur. J. Inorg. Chem. 1261 (2001).